ENHANCED KNOWLEDGE IN SCIENCES AND TECHNOLOGY
e-ISSN: 2773-6385

EKST

Vol. 5 No. 2 (2025) 80-89
https://publisher.uthm.edu.my/periodicals/index.php/ekst

Video Analysis of Vehicle Detection and Shadow Removal with Gaussian Mixture Model

Lim Jing Hong[1], Siti Suhana Jamaian[1]*

[1] *Department of Mathematics and Statistics, Faculty of Applied Sciences and Technology, UTHM Kampus Cawangan Pagoh Hub Pendidikan Tinggi Pagoh KM 1, Jalan Panchor, 84600 Pagoh, Muar, Johor, MALAYSIA.*

*Corresponding Author: suhana@uthm.edu.my
DOI: https://doi.org/10.30880/ekst.2025.05.02.011

Article Info

Received: 30 December 2024
Accepted: 18 January 2025
Available online: 19 December 2025

Keywords

Vehicle Detection, Gaussian Mixture Model, Shadow Removal

Abstract

Vehicle detection plays a vital role in Intelligent Transportation Systems (ITS). However, shadows present a significant challenge to the accuracy of traffic monitoring systems, often leading to the misclassification of shadows as vehicle components, distortion of object shapes, and compromised detection precision. Addressing this issue is crucial for enhancing the performance of ITS, as effective shadow detection and removal can improve vehicle detection accuracy, optimize traffic flow management, strengthen safety measures, and provide more reliable data for informed decision-making. This study proposes an improved approach to shadow removal that integrates the Gaussian Mixture Model (GMM) for vehicle detection with shadow removal using the HSV colour model, further refined by the Graph Cuts algorithm for improved segmentation. The video dataset used in this study is from the public Kaggle repository. The initial stage of shadow removal utilized the HSV colour model to process foreground features, followed by frame segmentation with Graph Cuts to eliminate residual shadow outlines, addressing the limitations of the colour model-based method. Comparative analysis revealed that incorporating Graph Cuts significantly enhanced shadow removal performance. The proposed algorithm achieved an average shadow detection rate of 92.10% without Graph Cuts and 98.25% with Graph Cuts. Furthermore, the method consistently maintained shadow discrimination rates exceeding 99% across all vehicle colours. These experimental results underscore the efficacy of the proposed framework in eliminating vehicle shadow outlines and enhancing the accuracy of vehicle detection, offering a robust solution for ITS applications.

1. Introduction

In recent years, roads have been an essential mode of transportation; there has been an annual increase in the number of events that occur on them worldwide [1]. Therefore, Intelligent Transportation Systems (ITS) for vehicle detection are receiving growing attention. ITS utilises advanced data transmission technologies to combine communication, computing, information, and other systems in the transportation industry [2]. To obtain accurate and reliable data, video analysis plays an important role in managing traffic and analysing traffic flow. This includes the use of technologies that can identify moving objects, track objects through a series of images, classify the tracked targets, and analyse the behaviours of objects [3].

The presence of shadows is one of the challenges to developing an effective traffic monitoring system [4]. When detecting moving vehicles, shadows are often incorrectly identified as part of the vehicle. This leads to the loss of objects or alteration of their shape, resulting in incorrect data. Addressing this issue is crucial for enhancing the performance of ITS, as effective shadow detection and removal can improve vehicle detection accuracy, optimize traffic flow management, strengthen safety measures, and provide more reliable data for informed decision-making.

Numerous methods have been conducted on object detection and shadow removal. Many researchers [5], [6], [7] and [8] have conducted an improved Gaussian Mixture Model (GMM) for vehicle detection. Their research findings proved to achieve higher accuracy in system detection and extract relevant moving target from the video. Several GMM-based approaches have been proposed to effectively identify and remove shadows from moving objects. [9] combined GMM with visual saliency maps; results indicate that it removes shadows and reduces the impact of camera jitter on moving objects. [10] improved the GMM by combining texture and colour features for shadow removal.

While colour models are also often used for shadow removal, notable examples include [4] and [8] studies using the HSV colour model in shadow removal for moving object detection. [11] proposed a cast shadow removal technique using YCbCr colour space shadow removal algorithm with optimised image segmentation using topological cuts. Some research utilising grayscale information is conducted by [3], [4] and [12]. Among the colour models, this study used the HSV colour model for its closer alignment with human perception of colour and its superior accuracy in distinguishing between objects and shadows.

This study focuses on determining vehicle detection using GMM and performing shadow removal of the vehicle using the HSV colour model. Moreover, it improves the performance of vehicle shadow removal with Graph Cuts. In this study cast shadows will be removed from the detected vehicle. The video sample included in this research is gathered from the available highway traffic recordings on Kaggle [13], focusing on outdoor highway traffic conditions during daytime under a clear sky. Vehicle detection and shadow removal methods are applied using OpenCV in Python programming language in Jupyter Notebook. The proposed method based on GMM and HSV colour space with Graph Cuts is expected to improve image segmentation and effectively remove shadow regions, thereby enhancing the accuracy of vehicle detection.

2. Methodology

This section presents methods for vehicle detection and shadow removal in video surveillance systems. Phase 1 involves the use of Gaussian Mixture Model (GMM) for detecting moving vehicles and updating the foreground frame. Phase 2 focuses on shadow removal, which is achieved through the implementation of an algorithm based on the HSV colour space. To enhance shadow removal accuracy, Phase 3 applies a Graph Cuts algorithm to the processed image. Lastly, the image output performance is analysed, and conclusions are made. All the processes in this study can be summarized as in flow chart in Fig. 1.

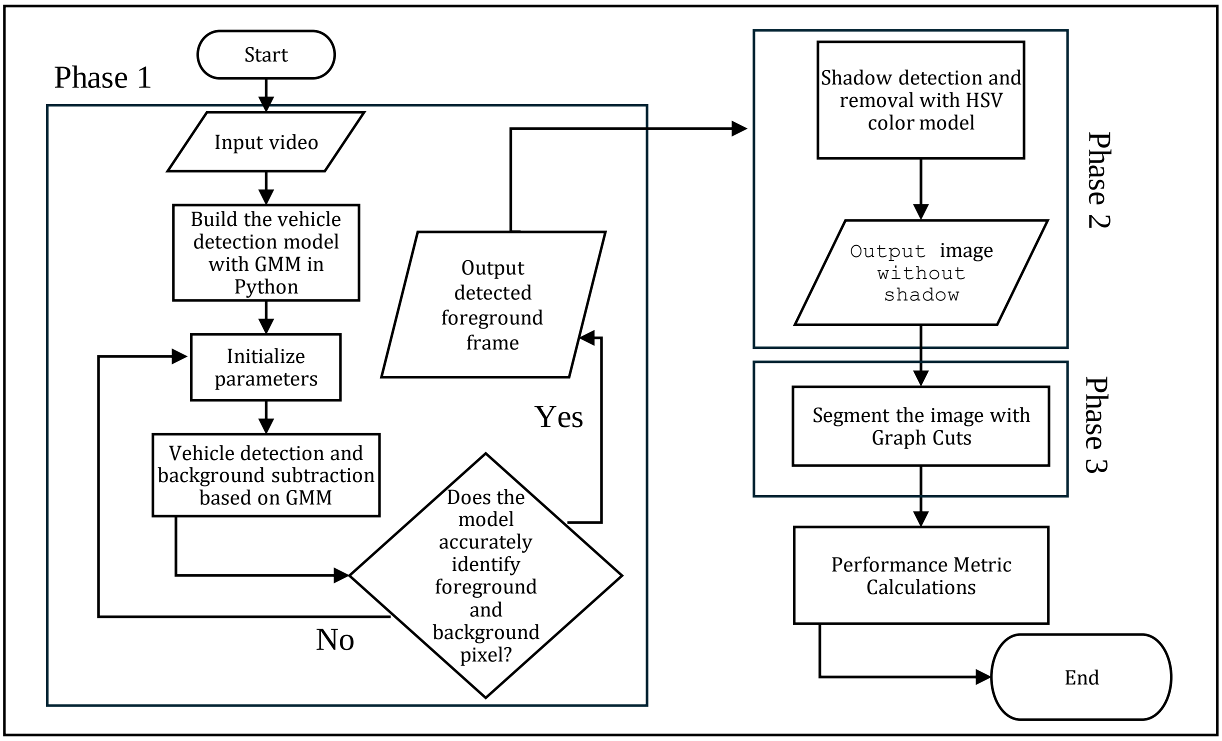

Fig. 1 Flowchart of the research methodology

2.1 Phase 1: Vehicle Detection

Gaussian Mixture Model (GMM) is implemented in background subtraction to detect vehicles in motion. Suppose the recent history of each pixel is $\{x_1, x_2, \ldots, x_t\}$, and the probability of identifying the current pixel value is defined as:

$$P(x_t) = \sum_{i=1}^{K} W_{i,t} \cdot \eta(x_t, \mu_{i,t}, \Sigma_{i,t}) \tag{1}$$

where K is the number of distributions. $\mu_{i,t}$ represents the mean value of the i-th Gaussian, $W_{i,t}$ represents an estimate of the weight of the i-th Gaussian in the mixture at time t, $\Sigma_{i,t}$ denotes the covariance matrix of the i-th Gaussian, and $\eta(x_t, \mu_{i,t}, \Sigma_{i,t})$ represents a Gaussian probability density function:

$$\eta(x_t, \mu_{i,t}, \Sigma_{i,t}) = \frac{1}{(2\pi)^{\frac{n}{2}} \cdot |\Sigma_{i,t}|^{\frac{1}{2}}} \cdot e^{-\frac{1}{2}(x_t-\mu_{i,t})^T \cdot \Sigma_{i,t}^{-1}(x_t-\mu_{i,t})} \tag{2}$$

where n indicates the pixel intensity dimension. The covariance matrix is assumed as follows:

$$\Sigma_{i,t} = \sigma_{i,t}^2 I \tag{3}$$

where I is the image sequences obtained at time t and $\sigma_{i,t}^{2}$ represents the variance of the i-th Gaussian at time t. The GMM assumes that the pixel values for RGB colour, that is red, green, and blue have equal variance and are mutually independent. This assumption can prevent the need for a computationally expensive matrix inversion up to a certain level of accuracy.

The process of estimating the background model begins by comparing each pixel value to the current Gaussian distribution value K and stops when a match is found. A pixel value that falls within a range of 2.5 standard deviations from the distribution is deemed to be a match. If the distribution of matches discovered for the new pixel value does not correspond to one of the background models, it is classified as the foreground. Otherwise, it is the background. As the background model, the B Gaussian distribution is selected and surpasses a specific threshold, expressed as:

$$B = argmin\left(\sum_{i=1}^{b} \mathrm{W}_i > Threshold\right) \tag{4}$$

The Gaussian models needed to be updated when it matched the current pixel. For the matched models, the parameters are updated as follows:

$$W_{i,t} = (1-\kappa)W_{i,t-1} + \kappa(N_{i,t}) \tag{5}$$
$$\mu_t = (1-\rho)\mu_{t-1} + \rho(x_t) \tag{6}$$
$$\sigma_t^2 = (1-\rho)\mu_{t-1}^2 + \rho(x_t-\mu_t)^T(x_t-\mu_t) \tag{7}$$

where κ is the learning rate and ρ is the second learning rate which is defined by:

$$\rho = \kappa \cdot \eta(x_t, \mu_i, \sigma_i) \tag{8}$$

If the model is a match, the value of $N_{i,t}$ is 1, while for the other models, it is 0. The mean and variance will remain the same, if the model is not matched. Once the weight is updated, the weight is then normalised. A new model is created if the current pixel does not correspond to any of the existing K Gaussian models. The Gaussian model with the lowest probability is substituted with a distribution that has the present value as its mean, a high initial variance, and a low current weight. The Gaussians are ranked by replacing the new value with $\frac{W}{\sigma}$. The value will rise when the distribution acquires additional evidence, and the variance decreases as reported in [14].

2.2 Phase 2: Shadow Removal

To achieve accurate segmented vehicle with no cast shadow, the HSV colour space is employed to detect and remove potential shadow pixels. HSV colour space accurately represents colours based on human perception, resulting in a more intuitive colour characterization. Hue (H) refers to the colour that commonly corresponds with a specific wavelength. Saturation (S) refers to the level of colour purity, which should fall between the highest level of purity (bright colour) and the absence of colour (grey level). The value (V) represents the measurement of colour light intensity and should fall within the range of absolute black and white [15]. The shadow detection's discriminative function is expressed as follows:

$$Sp(x,y) = \begin{cases} 1 & if\ \alpha \leq \dfrac{I_V(x,y)}{B_V(x,y)} \leq \beta \\ & and\ |I_S(x,y) - B_S(x,y)| \leq \tau_S \\ & and\ |I_H(x,y) - B_H(x,y)| \leq \tau_H \\ 0 & otherwise \end{cases} \tag{9}$$

where $I_H(x,y)$, $I_S(x,y)$ and $I_V(x,y)$ refers to the H, S, and V components of the current frame pixel, respectively. $B_H(x,y)$, $B_S(x,y)$ and $B_V(x,y)$ are the H, S, and V components of the background pixel. When $Sp(x,y)$ is 1, it indicates that the pixel is a shadow; otherwise, it belongs to the vehicle. τ_S and τ_H represent the threshold of difference between saturation and hue, respectively. α is associated with the intensity of shadow, and β is referred to the intensity of light as discussed in [16] and [17].

2.3 Phase 3: Graph Cuts

Lastly, Graph Cuts is applied to the final segmentation and refinement of the object contour. Graph Cuts involves an image represented as an array of grey values, denoted as $z = (z_1, \ldots, z_n, \ldots, z_N)$, where n is the index [18]. Each z_n represents a binary vector that indicates the assignments of pixel n in set N. Subsequently, the binary labels are assigned a value of 1 for the foreground and 0 for the background. The energy cost function $E(z)$ is defined by the equation:

$$E(z) = \alpha R(z) + B(z) \tag{10}$$

where $R(z)$ refers to the properties of the "region" of z and represents the penalties associated with assigning the pixel n to either the "object" or the "background". $B(z)$ represents the combined "boundary" characteristics and is understood as a penalty for lack of continuity between the pixels. α is an influencing component. The $E(z)$ represents the energy cost function, and the lowest value is achieved when all the pixels in the graph are categorised as either "object" or "background".

2.4 Evaluation Metrics

To measure the performance of the shadow detection method, two evaluation indicators proposed by [19] is applied: the shadow detection rate γ and shadow discrimination rate ξ, which are given as follows:

$$\gamma = \frac{TP_S}{TP_S + FN_S} \times 100\% \tag{11}$$

$$\xi = \frac{TP_F}{FN_F + TP_F} \times 100\% \tag{12}$$

where the subscript F stands for foreground and S for shadow. TP_S and TP_F, respectively, denote the number of true positive shadow pixels and foreground object pixels. Likewise, FN_s and FN_F, respectively, indicate the number of false negative shadow pixels and foreground object pixels [15].

2.5 Computational Algorithm

The Gaussian mixture model algorithm has been implemented to detect moving vehicles in a video. A video is inputted into the algorithms and extracted as frames for further processing. In each video frame, the foreground of the moving vehicle is obtained. Furthermore, the frame is converted to HSV colour space to remove the moving vehicle's shadow. The shadow region is detected and removed by defining the HSV values range in these shadow regions. Graph Cuts is an image segmentation technique. Initially, we draw a rectangle around the foreground region. Everything outside the rectangle will be recognized as background. Then, the algorithm segments the foreground object iteratively to obtain the outcome. The Graph Cuts was added to the algorithm to increase shadow removal performance further. The steps are as follows:

Phase 1: *Vehicle detection*
Step 1: Define parameters for the Gaussian Mixture Model (GMM) to separate foreground (vehicles) and background.
Step 2: The GMM was applied to identify foreground and background regions for each frame

Step 3: Morphological operation is applied to clean up the noise in the foreground mask
Step 4: Save the cleaned-up foreground frame as an output image.
Step 5: Read the next frame and steps 2 to 4 were repeated. Stop when no more frames are available.
Phase 2: *Shadow removal*
Step 6: Frames with clear visibility and minimal motion blur were selected
Step 7: A rectangular bounding box is drawn tightly around the selected foreground object (vehicle) with a shadow in each selected frame
Step 8: The frame is converted from RGB to HSV color space for shadow detection
Step 9: HSV thresholds (lower and upper bounds) were defined to identify shadow regions.
Step 10: Detected shadow regions were subtracted from the foreground mask (Phase 1) to isolate the foreground object without shadows.
Phase 3: *Improving Accuracy with Graph Cuts*
Step 11: Shadow-free frames from Phase 2 is selected for further refinement.
Step 12: A rectangular bounding box is drawn tightly around the selected foreground object (vehicle) without shadow in each selected frame.
Step 13: Graph Cuts algorithm is applied to enhance the accuracy of the shadow removal.
Step 14: The refined foreground object is saved as the final output.
Step 15: Steps 12 to 14 are repeated for other selected frames.

3. Results and Discussion

This study uses the Gaussian Mixture Model (GMM) to detect moving vehicles. HSV colour model is used to identify shadows. Then, the outcome is further improved by applying Graph Cuts. The effectiveness of the proposed method in identifying moving vehicles and shadow removal in different car colours is demonstrated. Additionally, comparisons are conducted to evaluate the improvements in detection when the Graph Cuts is applied.

3.1 Performance of Different Vehicle Colours

In this study, an investigation of a traffic monitoring video dataset retrieved from Kaggle [13] is performed to evaluate the proposed method. Vehicle detection will first be conducted using the Gaussian Mixture Model (GMM) and producing a binary frame where the moving foreground will become white, whereas the background will be black. Fig. 2(a) shows the original frame before GMM. Fig. 2(b) shows the binary map of the foreground object detected using GMM.

(a) (b)

Fig. 2 (a) Original frame72 retrieved from Kaggle [13]; (b) Binary map of the foreground object

Before conducting the shadow removal on the vehicle, a rectangular bounding box is drawn to isolate a specific vehicle colour within the frame to focus on its binary map and exclude irrelevant regions. A white car in Fig. 3(a) has been selected to evaluate the performance of the proposed shadow removal method as shown in Fig. 3. GMM is then applied to detect the white vehicle from the video and generate a binary map frame, as illustrated in Fig. 3(b). The binary map of the shadow region is determined using the HSV colour model, as shown in Fig. 3 (c). Finally, the shadow region is removed by subtracting it from the foreground. The final binary map of the white car, following shadow removal, is presented in Fig. 3(d).

(a) (b) (c) (d)

Fig. 3 (a) Original frame; (b) Detected foreground; (c) Binary map of shadow region; (d) Binary map after shadow removal

The process of shadow removal is applied uniformly across vehicles with different colours, following the same steps and methodology. This study evaluates shadow removal in vehicles using Kaggle video datasets. The colours, including white, silver, red, green, beige, silvery blue, dark pink, blue, dark blue, dark red, and black, are listed in ascending order of brightness value, starting from the lighter colour and progressing to the darker colour. Shadow detection rate (11) measures the accuracy of an algorithm in identifying shadow pixels, while the shadow discrimination rate (12) measures the correct classification of non-shadow regions. In Table 1, the result for each respective vehicle colour is shown. Table 2 shows the result of shadow removal performance for each respective vehicle colour.

Table 1 Result for a vehicle after shadow removal

Vehicle Colour	Foreground object	Foreground object after shadow removal	Vehicle Colour	Foreground object	Foreground object after shadow removal
White		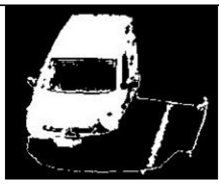	Dark pink		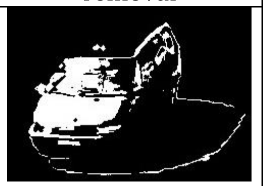
Silver		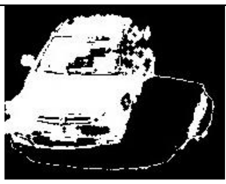	Blue		
Red		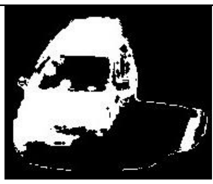	Dark blue		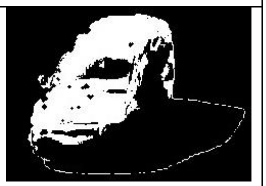
Green		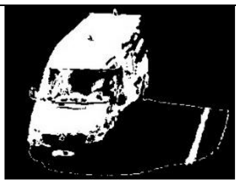	Dark red		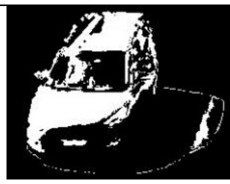
Beige		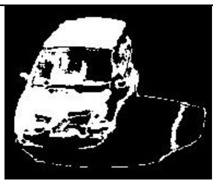	Black		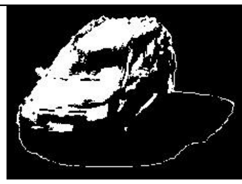
Silvery blue		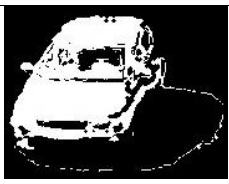			

Table 2 Shadow removal performance result

Vehicle Colours	Shadow detection rate (γ)	Shadow discrimination rate (ξ)
White	0.8904	0.9964
Silver	0.8998	0.9986
Red	0.9026	0.9964
Green	0.9033	0.9914
Beige	0.9248	0.9970
Silvery blue	0.9545	0.9975
Dark pink	0.9438	0.9934
Blue	0.8756	0.9991
Dark blue	0.9551	0.9938
Dark red	0.9257	0.9937
Black	0.9559	0.9927

Based on Table 2, all darker-coloured vehicles have higher shadow detection rates compared to lighter vehicles' colours, are likely due to shadows creating a reduction in light. On darker surfaces, this reduction is more pronounced because there is a heightened contrast between the shadow and the darker colour of the car. However, blue as a darker coloured has the lowest shadow detection rate due to its specific tone blending with the shadow regions. Observing Table 1, dark blue and dark pink vehicles notably suffered the most significant vehicle form loss due to their colour similarity to the grey shadow, resulting in partial removal. All colour vehicles performed with high shadow discrimination rates, with values consistently above 99%. Moreover, despite the high discrimination rates, there are still some residual shadow outlines in the images.

3.2 Performance of Different Vehicle Colours with Graph Cuts

The disadvantage of traditional shadow removal using colour space is that it often leaves the residual outlines of shadows, which can negatively impact the quality and accuracy of the processed image. To address this problem, the Graph Cuts algorithm is used to segment the result to remove the shadow outline.

The process of Graph Cuts is illustrated in Fig. 4. Fig. 4(a) is the binary map result of the white car derived from the preceding shadow removal process in Fig. 3(d). Subsequently, a bounding box is manually defined by the user according to the location of the white car within the frame. This bounding box is illustrated as a green rectangle in Fig. 4(b), while the foreground object is highlighted in yellow by the Graph Cuts algorithm. The shadow region extracted during the process is illustrated in Fig. 4(c), while Fig. 4(d) shows the final output of the shadow removal process with the Graph Cuts algorithm.

(a) (b) (c) (d)

Fig. 4 (a) Binary map after shadow removal; (b) Segmentation with Graph Cuts; (c) Shadow region extracted with Graph Cuts; (d) Binary map after shadow removal with Graph Cuts

The results of shadow removal, as documented in Table 1, are incorporated into Table 3 under the column representing the foreground object without the application of the Graph Cuts for comparison purposes. The results clearly indicate that the post-processed output, achieved through Graph Cuts, exhibits a cleaner appearance with the removal of shadow outlines. The results of the comparative analysis are presented in Table 4. The difference in shadow detection rate is calculated by subtracting the shadow detection rate (with the Graph Cuts) from the shadow detection rate (without the Graph Cuts).

Table 3 Result for vehicle shadow removal with Graph Cuts

Vehicle Colour	Foreground object without Graph Cuts	Foreground object with Graph Cuts	Vehicle Colour	Foreground object without Graph Cuts	Foreground object with Graph Cuts
White	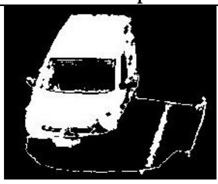	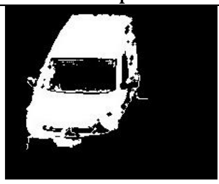	Dark pink	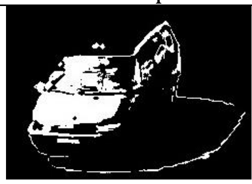	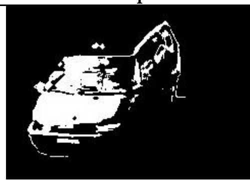
Silver			Blue		
Red		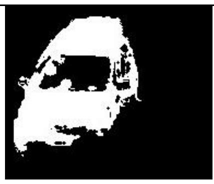	Dark blue	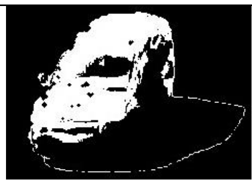	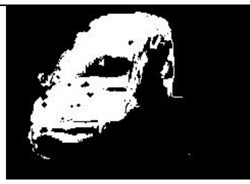
Green	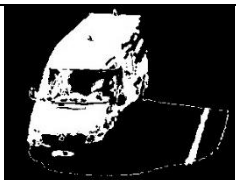	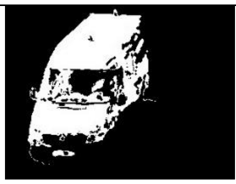	Dark red	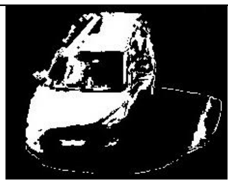	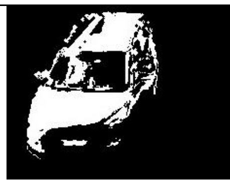
Beige	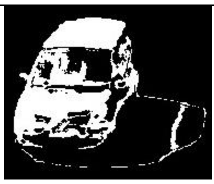	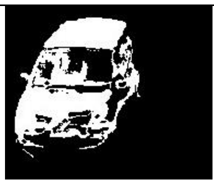	Black	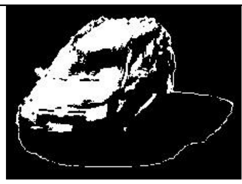	
Silver blue	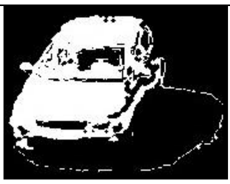				

Let γ_1 be the shadow detection rate without Graph Cuts as from Table 2, whereas γ_2 is the new shadow detection with the application of Graph Cuts. Based on Table 4, the calculated difference $\gamma_2 - \gamma_1$, reveals that the shadow detection rate improved across all vehicle colours. The Graph Cuts algorithm demonstrated its effectiveness in refining the shadow removal process, regardless of whether the colour is darker or lighter.

Conversely, the shadow discrimination rates remain unchanged with the Graph Cuts, indicating that the removed shadow outlines are part of the shadow region rather than non-shadow areas. It is evident that incorporating Graph Cuts improves the accuracy of shadow removal.

Table 4 Shadow removal performance comparison with and without Graph Cuts

Vehicle Colours	Without Graph Cuts	With Graph Cuts	Difference in shadow detection rate
	γ_1	γ_2	$\gamma_2 - \gamma_1$
White	0.8904	0.9816	0.0912
Silver	0.8998	0.9852	0.0854
Red	0.9026	0.9865	0.0839
Green	0.9033	0.9736	0.0703
Beige	0.9248	0.9861	0.0613
Silvery blue	0.9545	0.9860	0.0315
Dark pink	0.9438	0.9906	0.0468
Blue	0.8756	0.9586	0.0830
Dark blue	0.9551	0.9854	0.0303
Dark red	0.9257	0.9856	0.0599
Black	0.9559	0.9880	0.0321

4. Conclusion

Traffic monitoring has long been a critical application in transportation planning and engineering, serving to extract valuable and accurate traffic data for traffic image classification and flow control. Effective vehicle detection necessitates the removal of shadows cast by vehicles. This study proposed a shadow removal method based on the Gaussian Mixture Model (GMM) and enhanced using HSV colour space combined with the Graph Cuts algorithm to improve shadow detection and removal. The proposed approach has been shown to be effective in achieving high shadow detection and discrimination rates. Compared to lighter vehicles, all darker-coloured vehicles have higher shadow detection rates, which is mainly due to the reduction of shadows, making darker surfaces more noticeable. The results from the investigation, as demonstrated in Table 4, show an increase in shadow detection rate when comparing the method without Graph Cuts to the method with Graph Cuts, highlighting the method's robustness and effectiveness in shadow removal. Consequently, all objectives of the study were successfully achieved.

However, the Graph Cuts method has certain limitations. It assumes the presence of a single foreground object within a specified rectangular region, rendering it unsuitable for scenarios involving multiple distinct objects, such as frames containing multiple vehicles. Additionally, its performance is highly dependent on the accuracy of the initial bounding box, which may compromise results if the bounding box is inaccurately defined.

A recommendation for future work is to develop a more automated and real-time method for vehicle shadow removal to achieve more robust results. Moreover, future studies should consider exploring the combined characteristics of road surfaces and shadows, as this could provide a deeper understanding and refinement of shadow removal methodologies.

Acknowledgement

The authors would like to thank the Faculty of Applied Sciences and Technology, Universiti Tun Hussein Onn Malaysia for its support.

Conflict of Interest

Authors declare that there is no conflict of interests regarding the publication of the paper.

Author Contribution

The authors confirm contribution to the paper as follows: ***study conception and design:*** *Lim Jing Hong, Siti Suhana Jamaian;* ***analysis and interpretation of results:*** *Lim Jing Hong;* ***validation of results:*** *Siti Suhana Jamaian;* ***draft manuscript preparation:*** *Lim Jing Hong, Siti Suhana Jamaian. All authors reviewed the results and approved the final version of the manuscript.*

References

[1] A. Pramanik, S. Sarkar, and J. Maiti, "A Real-time Video Surveillance System for Traffic Pre-events Detection. Accident Analysis and Prevention," *Accident Analysis & Prevention*, vol. 154, pp. 106019, May 2021, doi: 10.1016/j.aap.2021.106019.

[2] S. A. Sayed, Y. Abdel-Hamid, and H. A. Hefny, "Artificial Intelligence-based Traffic Flow Prediction: A Comprehensive Review," *Journal of Electrical Systems and Information Technology*, vol. 10, no. 1, pp. 13–55, Mar. 2023, doi: 10.1186/s43067-023-00081-6.

[3] P. Kumar, S. Ranganath, H. Weimin, and K. Sengupta, "Framework for Real-time Behavior Interpretation from Traffic Video," *IEEE Transactions on Intelligent Transportation Systems*, vol. 6, no. 1, pp. 43–53, Mar. 2005, doi: 10.1109/TITS.2004.838219.

[4] H. N. Phan, L. Hoang Pham, N. M. Chung and S. Viet-Uyen Ha, "Improved Shadow Removal Algorithm for Vehicle Classification in Traffic Surveillance System," *2020 RIVF International Conference on Computing and Communication Technologies (RIVF)*, Ho Chi Minh City, Vietnam, 2020, pp. 1–6, doi: 10.1109/RIVF48685.2020.9140784.

[5] Indrabayu, R. Y. Bakti, I. S. Areni and A. A. Prayogi, "Vehicle detection and tracking using Gaussian Mixture Model and Kalman Filter," *2016 International Conference on Computational Intelligence and Cybernetics, Makassar*, Indonesia, 2016, pp. 115-119, doi: 10.1109/CyberneticsCom.2016.7892577.

[6] J. Zuo, Z. Jia, J. Yang and N. Kasabov, "Moving Target Detection Based on Improved Gaussian Mixture Background Subtraction in Video Images," in *IEEE Access*, vol. 7, pp. 152612-152623, Oct. 2019, doi: 10.1109/ACCESS.2019.2946230.

[7] Z. Tang and Z. Miao, "Fast Background Subtraction Using Improved GMM and Graph Cut," *2008 Congress on Image and Signal Processing,* Sanya, China, 2008, pp. 181-185, doi: 10.1109/CISP.2008.459.

[8] B. K. Yadav and J. Xiaogang, "An Algorithm for Intelligent Identification of Moving Objects in Natural Environment," *International Journal of Machine Learning and Computing*, vol. 10, no. 5, pp. 637–647, Oct. 2020, doi: 10.18178/ijmlc.2020.10.5.985.

[9] L. L. Lin and N. R. Chen, "Moving Objects Detection Based on Gaussian Mixture Model and Saliency Map," in *Advanced Research on Mechanical Engineering, Industry and Manufacturing Engineering*, vol. 63, *Applied Mechanics and Materials*, Trans Tech Publications Ltd, Aug. 2011, pp. 350–354, doi: 10.4028/www.scientific.net/AMM.63-64.350.

[10] J. Ding and G. Zhao, "Gray Sequence Image Shadow Removal Algorithm Based on Computer Vision," *2020 12th International Conference on Measuring Technology and Mechatronics Automation (ICMTMA)*, Phuket, Thailand, 2020, pp. 366–370, doi: 10.1109/ICMTMA50254.2020.00087.

[11] Q. Shao, C. Xu, Y. Zhou, and H. Dong, "Cast shadow detection based on the YCbCr color space and topological cuts," *The Journal of Supercomputing*, vol. 76, no. 5, pp. 3308–3326, May 2020, doi: 10.1007/s11227-018-2558-4.

[12] S. Vikruthi, M. Archana, and R. C. Tanguturi, "Shadow detection and elimination technique for vehicle detection," *Revue d'Intelligence Artificielle*, vol. 36, no. 5, pp. 753–760, Dec. 2022, doi: 10.18280/ria.360513.

[13] F. Nekouei, 2023, "Top view vehicle detection image dataset," Kaggle. [Online]. Available: https://www.kaggle.com/datasets/farzadnekouei/top-view-vehicle-detection-image-dataset

[14] N. A. Mohd Aris and S. S. Jamaian, "Background subtraction challenges in motion detection using Gaussian mixture model: a survey," *IAES International Journal of Artificial Intelligence (IJ-AI)*, vol. 12, no. 3, pp. 1007–1018, Sep. 2023, doi: 10.11591/ijai.v12.i3.pp1007-1018.

[15] B. Farou, H. Rouabhia, H. Seridi, and H. Akdag, "Novel approach for detection and removal of moving cast shadows based on RGB, HSV and YUV color spaces," *Computing and Informatics*, vol. 36, no. 4, pp. 837–856, Jan. 2017, doi: 10.4149/cai_2017_4_837.

[16] M. Wu, C. Rui, and Y. Tong, "Shadow elimination algorithm using color and texture features," *Computational Intelligence and Neuroscience*, vol. 2020, no. 1, pp. 1–10, Jan. 2020, doi: 10.1155/2020/2075781.

[17] H. Zhang, S. Qu, H. Li, J. Luo and W. Xu, "A Moving Shadow Elimination Method Based on Fusion of Multi-Feature," in *IEEE Access*, vol. 8, pp. 63971-63982, 2020, doi: 10.1109/ACCESS.2020.2984680.

[18] C. Rother, V. Kolmogorov, and A. Blake, ""GrabCut"-Interactive Foreground Extraction using Iterated Graph Cuts," *ACM Trans. Graph.*, vol. 23, no. 3, pp. 309-314, Aug. 2004, doi: 10.1145/1015706.1015720.

[19] A. Prati, I. Mikic, M. Trivedi, and R. Cucchiara, "Detecting moving shadows: Algorithms and evaluation," *IEEE Transactions on Pattern Analysis and Machine Intelligence*, vol. 25, no. 8, pp. 918–923, Aug. 2003, doi: 10.1109/TPAMI.2003.1206520.